



Published in final edited form as:

*J Comput Assist Tomogr.* 2014 ; 38(4): 526–534. doi:10.1097/RCT.0000000000000053.

## EFFECT OF PRE-ENHANCEMENT SET-POINT ON CT PERFUSION VALUES IN NORMAL LIVER AND METASTASES TO THE LIVER FROM NEUROENDOCRINE TUMORS

Chaan S. Ng, MD<sup>1</sup>, Adam G. Chandler, PhD<sup>2,5</sup>, James C. Yao, MD<sup>3</sup>, Delise H. Herron, BS<sup>1</sup>, Ella F. Anderson, RT<sup>1</sup>, Chusilp Charnsangavej, MD<sup>1</sup>, and Brian P. Hobbs, PhD, MS<sup>4</sup>

<sup>1</sup>Department of Diagnostic Radiology, The University of Texas MD Anderson Cancer Center, Houston, Texas

<sup>2</sup>Department of Imaging Physics, The University of Texas MD Anderson Cancer Center, Houston, Texas

<sup>3</sup>Department of Gastrointestinal Medical Oncology, The University of Texas MD Anderson Cancer Center, Houston, Texas

<sup>4</sup>Department of Biostatistics, The University of Texas MD Anderson Cancer Center, Houston, Texas

<sup>5</sup>CT research, GE Healthcare, Waukesha, Wisconsin

### Abstract

**Objective:** To assess the effects of pre-enhancement setpoint ( $T_1$ ) positioning on CT perfusion (CTp) parameter values.

**Methods:** CTp in 16 patients with neuroendocrine liver metastases were analyzed by distributed parameter modeling to yield tissue blood flow (BF), blood volume (BV), mean transit time (MTT), permeability (PS), and hepatic arterial fraction (HAF), for tumor and normal liver, with displacements in  $T_1$  of  $\pm 0.5s$ ,  $\pm 1.0s$ ,  $\pm 2.0s$ , relative to gold-standard. A linear mixed-effects model was used to assess the displacement effects.

**Results:** Effects on CTp parameter values were variable: BF was not significantly affected, but  $T_1$  positions of  $+1.0s$  and  $-2.0s$  significantly affected the other CTp parameters ( $p < 0.004$ ). Mean differences in CTp parameter values versus gold-standard for BF, BV, MTT, PS and HAF ranged from  $-5.0$  to  $5.2\%$ ,  $-12.7$  to  $8.9\%$ ,  $-12.5$  to  $8.1\%$ ,  $-5.3$  to  $5.7\%$ , and  $-12.9$  to  $26.0\%$ , respectively.

**Conclusions:** CTp parameter values can be significantly affected by  $T_1$  positioning.

### INTRODUCTION

Computed tomography perfusion (CTp) is a technique with the ability to noninvasively assess and quantify tissue perfusion. It has a variety of potential applications in oncologic imaging, including treatment monitoring, prognostication and pathophysiological

interrogation.<sup>1-4</sup> In this arena, the technique has been utilized in a range of organ systems and tumors, including head and neck,<sup>5-7</sup> pelvis,<sup>8-14</sup> thorax,<sup>15-17</sup> and abdomen,<sup>18,19</sup> the latter including the liver.<sup>20-23</sup>

Analysis of CTP data is able to yield a variety of perfusion parameters, depending on the particular physiological model that is used to describe the behavior of tissue perfusion. One model that is widely applied is based on an adiabatic approximation of the distributed parameter model.<sup>24</sup> In this method, tissue and vascular input time-attenuation curves, obtained from cine or semi-continuous CT acquisition data during intravenous (IV) administration of contrast medium, are deconvoluted. Estimates of tissue blood flow (BF), blood volume (BV), mean transit time (MTT), and permeability-surface area product (PS) can then be derived.<sup>25</sup> In the particular setting of liver perfusion, two vascular input functions need to be considered, arterial and portal venous; and in addition, hepatic arterial fraction (HAF) can be derived.<sup>26</sup>

The deconvolution process is critically dependent on the two or, in the case of liver, three time-attenuation curves above. One important factor in defining these curves is the delineation of the pre-enhancement setpoint, or time/image at which the arterial up-slope is considered to first occur. This is a user-defined variable and is inevitably subject to observer variations. There have only been a few studies which have investigated the potential effects of the positioning of the pre-enhancement setpoint on CTP parameter values using distributed parameter modeling, for example Sanelli et al,<sup>27</sup> which involved the brain. To the best of our knowledge, there have been no studies which have systematically assessed its impact in tumors or tissues in abdominal locations. The liver is a common site of tumors, and hence an important organ system to gain an understanding of the factors that may affect quantification of perfusion parameters. The objective of this study was to evaluate the effects of the positioning of the pre-enhancement setpoint on CTP parameter values in normal liver and in metastases to the liver from neuroendocrine tumors.

## MATERIALS AND METHODS

### Patients

CTp data for this study was obtained from two prospective treatment protocols for patients with metastatic neuroendocrine tumors who had been treated with bevacizumab (a VEGF inhibitor), everolimus (an mTOR inhibitor), or pazopanib (an inhibitor of VEGFR), and in which CTP had been offered as an optional study for patients. The current retrospective study was approved by our institutional review board (IRB), with waiver of informed consent. The study complied with HIPAA regulations.

The current study focused on patients in whom CTP had been undertaken on a target lesion in the liver. Proof of malignancy by biopsy of the target lesion was considered excessively invasive, but all lesions were clinically or radiologically considered malignant, based on biopsy of other lesions, widespread metastatic disease and/or increase in size of lesions. A single target lesion had been identified on review of previous imaging studies in each patient by a radiologist (C.S.N. with more than 10 years' experience in interpreting CT studies).

The primary target lesions were required to be well-demarcated, contrast-enhancing solid masses larger than 2.5 cm in longest diameter.

### CT Perfusion Scanning Technique

Patients underwent CTP scanning in the supine position. Images were obtained by using a 64-row multidetector CT scanner (VCT, GE Healthcare, Waukesha, WI). The scans were obtained in two phases: Phase 1, cine acquisition during a breath-hold, followed by Phase 2, consisting of eight intermittent short breath-hold helical scans (outlined in Figure 1). A localization, inspiratory breath-hold, helical scan without IV contrast was first obtained to identify the CT coordinates of the target lesion, as follows: tube voltage, 120 kV; tube current, 320 mA; slice thickness, 5 mm; slice interval, 5 mm; pitch factor, 0.969:1; speed 19.37; rotation speed, 0.8 second; field of view, 32–40 cm; and matrix, 512 × 512.

After the localization image, Phase 1 (“cine”) scans were performed using a single level of 4 cm thickness (0.5-cm contiguous slice thickness for eight slices, 8i cine mode) at the midpoint of the target lesion, as follows: tube voltage, 120 kV; tube current, 90 mA; field of view, 32–40 cm; matrix, 512 × 512. Images were obtained during a 30-second inspiratory breath-hold. Data acquisition started 5 seconds after intravenous injection of 50 mL of a nonionic contrast agent (ioversol [Optiray], 320 mg of iodine/100 mL; Mallinckrodt, Inc., St. Louis, MO) using an automatic injector (MCT/MCT Plus; Medrad, Pittsburgh, PA) and an injection rate of 7 mL/second. Images were reconstructed every half second.

Phase 2 (“delayed”) scans were eight intermittent short 3.6s inspiratory breath-hold helical scans, as follows: tube voltage, 120 kV; tube current, 90 mA; slice thickness, 5 mm; slice interval, 5 mm; pitch factor, 0.984:1; speed 39.37; rotation speed, 0.8 second. The first Phase 2 helical scan commenced 20 seconds after the end of the Phase 1 acquisition; the subsequent seven helical scans were obtained at increasing intervals as illustrated in Figure 1 (top row). The final helical acquisition commenced 590 seconds after the start of Phase 1 acquisition. Images were reconstructed to 5mm thickness. The estimated effective dose for this CTP protocol was 28 mSv.

When required for clinical purposes, the CTP study was followed by routine staging CT scans of chest, abdomen, and/or pelvis, using intravenous administration of a further 100 mL of contrast medium.

### CT Perfusion analyses

In order to have the most robust data for our analysis, we only utilized CTP datasets in which there was negligible motion in the Phase 1 images since this removed the need to anatomically register the Phase 1 images. The Phase 2 images of each selected patient dataset were then anatomically registered with the corresponding Phase 1 images using a semi-automated rigid registration algorithm.<sup>28,29</sup> This resulted in CTP datasets consisting of fifty-nine 8-slice cine images temporally sampled at 0.5s from the Phase 1 acquisition, together with eight anatomically matched 8-slice images from the Phase 2 acquisition, which formed the reference dataset for subsequent analyses.

The above reference datasets were analyzed using the Liver Protocol of a commercially available CTP platform (CT Perfusion 4 version 4.3.1, Advantage Windows 4.4; GE Healthcare, Waukesha, WI). Regions of interest (ROI) were placed in the abdominal aorta and in the portal vein on the source images to provide the dual vascular inputs required in the Liver specific protocol (C.S.N.) (Figure 2a, 2b). Three setpoints were then delineated: a *pre-enhancement* setpoint ( $T_1=0s$ ), which corresponded to the time when the arterial signal first began to rise; a *post-enhancement* setpoint ( $T_2$ ), which corresponded with the final time point of the Phase 1 data acquisition; and the *last second phase* setpoint ( $T_3$ ), which corresponds to the final Phase 2 image (Figure 1, first row; Figure 2a). Perfusion parametric maps were generated of blood flow (BF), blood volume (BV), mean transit time (MTT), permeability–surface area product (PS) values, and hepatic arterial fraction (HAF).

For each of the axial slice locations in which the primary tumor was identified, an ROI was drawn freehand around the periphery of the lesion, using an electronic cursor and mouse, with reference to the source cine CT images (width = 350 HU, level = 40 HU) and perfusion maps. Wherever possible, a second tumor ROI was delineated, provided it was greater than 1.5 cm in diameter (E.F.A and D.H.H in consensus, each with greater than 15 years' experience in CT perfusion analyses).

Circular or oval ROIs were delineated in normal liver regions to enable parallel analyses of normal liver parenchyma; these ROIs were as large as possible and placed to avoid vessels and artifacts. We delineated two normal liver ROIs on each of the 8 slices; and wherever possible, separate ROIs were placed in the left and right liver lobes (C.S.N.) (Figure 2a).

Average tissue BF, BV, MTT, PS and HAF values were obtained from the CT levels in which tumor and normal liver ROIs were drawn, and the mean values across all CT levels were computed. All ROIs were saved within the software to enable identical placement in all the subsequent analyses.

CTp parameter values with varying acquisition duration were obtained by repeating the above analyses with systematic reductions in the post-enhancement setpoints between 590s and 12s: firstly, by sequential reductions of  $T_3$  within the Phase 2 data (i.e., 590s to 50s) (Figure 1, second row); and secondly, by sequential 2s reductions of  $T_2$  within the Phase 1 data (i.e., 30s to 12s) (Figure 1, third and fourth rows). These were all undertaken with  $T_1$  fixed at the time point determined in the above reference dataset (i.e., with  $T_1=0s$ ).

### Effect of pre-enhancement setpoint

The above analyses were repeated with varying pre-enhancement setpoints ( $T_1$ ). These analyses were undertaken using the same arterial, portal venous and tissue ROIs as used in the corresponding reference analyses.

In order to determine an appropriate range of pre-enhancement setpoints to evaluate, we undertook a preliminary pilot study to assess the variability of observers in determining pre-enhancement positions. In this pilot study, four observers (E.F.A, A.G.C, D.H.H, C.S.N) identified and recorded the positions of their pre-enhancement setpoints, independently and on 2 occasions separated by at least 4 weeks, in 24 arterial input functions from CTP

datasets which had been obtained in a similar manner to the current study. This preliminary study indicated a standard deviation in the pre-enhancement position compared to the average of all data (arbitrarily set at zero), of 0.55s, with a range of  $-1.8$ s to  $+1.5$ s.

In the light of these results, and to allow for a comprehensive analysis, we undertook the CTP analyses with relative displacements in  $T_1$  as follows:  $-2.0$ s,  $-1.0$ ,  $-0.5$ s,  $+0.5$ s,  $+1.0$ s, and  $+2.0$ s relative to  $T_1=0$ s (Figure 1, fifth and sixth rows).

## Statistical Analysis

**Effect of pre-enhancement setpoint on CTP parameter stabilization times**—In a previous analysis of the reference subset of  $T_1=0$ s, it was observed that CTP parameter values approached steady-state (equilibrium or time-invariant) values with increasing confidence (“low”, “moderate” and “high”) with increasing acquisition durations (12s to 590s).<sup>30</sup> The same statistical model and method of inference was applied in the current analysis to evaluate the effects of pre-enhancement displacement on stabilization with acquisition duration, for  $T_1$  varying from  $-2$ s to  $+2$ s. Details of the statistical model and method of inference have been presented previously (Appendix 2 in the above article<sup>30</sup>).

**Effect of pre-enhancement setpoint on CTP parameter values**—A linear mixed-effects model was used to accommodate the nested structure of the data. For each tissue type and acquisition duration each patient contributed one or two sets of CTP parameter values obtained under seven pre-enhancement setpoints observed within one or two disparate ROIs. Random intercepts were used to account for the inherent inter-patient and intra-patient, inter-ROI sources of variation, inducing compound symmetric covariance structure among clustered observations within the same patient and ROI. The model was used to conduct inference on six adjustment factors characterizing the effects of each of the six pre-enhancement displacement ( $T_1 = \pm 0.5$ s,  $\pm 1.0$ s,  $\pm 2.0$ s) on resultant CTP parameter values in relation to the reference setpoint ( $T_1=0$ s). The approach obviates assumptions of linear displacement trends. Adjustment for multiple comparisons used Bonferroni’s correction, resulting in a significance threshold of  $p < 0.0083$ . Data from tumor and normal liver were analyzed separately. The statistical software R (R Development Core Team, <http://www.r-project.org>) version 2.12.2 with package “nlme” was used for statistical analysis.

## RESULTS

The study cohort consisted of 16 patients with metastases to the liver from neuroendocrine tumors. The median age of the patients was 57.5 years (range, 42.0 to 69.7 years), with 6 male and 10 female patients.

There were 25 separate tumor ROIs, as follows: 18 from 9 patients who each had 2 tumor ROIs, and 7 from patients who had one tumor ROI. There were 27 normal liver ROIs, as follows: 24 from 12 patients who each had normal liver ROIs in the right hepatic lobe and the left lobe; 3 from patients who had both their normal liver ROIs in the right lobe (which were then averaged). One patient did not have delineable normal liver parenchyma on the available CTP images.

### Effect of pre-enhancement setpoint on CTP parameter stabilization times

The levels of confidence in stability (“low”, “moderate” and “high”) of CTP parameter values attained at various acquisition times for  $T_1 = 0s$  and  $\pm 2.0s$ , for tumor and normal liver, are presented in Table 1. This shows that the levels of confidence in stabilization of CTP values attained with specific acquisition times were substantially the same across the range in pre-enhancement displacements evaluated, and that the pattern of behavior for tumor and normal liver were essentially the same. At least 160s was required to attain at least low confidence in stability for the majority of CTP parameters. Increasing levels of confidence were attained with increasing acquisition durations, from 160s through 360s. With an acquisition time of 220s, it was observed that at least low confidence in stabilization was attained for all CTP parameters, with moderate confidence for the majority of CTP parameters. With an acquisition time of 360s, at least moderate confidence in stabilization was attained for all CTP parameters, with high confidence for the majority. There was no additional improvement in confidence across the parameters with 590s acquisition duration compared to 360s. PS did not attain a high confidence of stabilization within the 590s of available acquired data.

### Effect of pre-enhancement setpoint on CTP parameter values

Detailed analyses and comparisons of varying pre-enhancement displacements were limited to two specific acquisition durations, specifically, 220s and 360s, since at these times at least moderate and high levels of confidence in stabilization of CTP values were attained across the majority of parameters, respectively. Scatterplots of the observed CTP parameters values for the range of pre-enhancement displacements analyzed are presented in Figure 3. A summary of CTP parameter values obtained for the reference pre-enhancement setpoint ( $T_1=0s$ ) analyzed at the designated acquisition durations of 220s and 360s are presented in Table 2.

The relative differences in resultant CTP values, compared to the reference pre-enhancement setpoint ( $T_1=0s$ ), as a function of displacement ( $T_1 = \pm 0.5s, \pm 1.0s, \pm 2.0s$ ), after 220s and 360s of acquisition, are presented in Table 3. For the 360s analyses, mean differences in CTP parameter values compared to reference values for BF, BV, MTT, PS and HAF, ranged from  $-5.0\%$  to  $+5.2\%$ ,  $-12.7\%$  to  $+8.9\%$ ,  $-12.5\%$  to  $+8.1\%$ ,  $-5.3\%$  to  $+5.7\%$ ,  $-12.9\%$  to  $+26.0\%$ , respectively. The ranges in mean differences for the 220s analyses were similar.

Formal statistical testing of these differences at the various pre-enhancement displacements compared to  $T_1=0s$  are presented in Table 4, and graphically in Figure 4. Variations in  $T_1$  positions were found to affect the resultant CTP values compared to reference values to different degrees. For all five CTP parameters,  $T_1$  displacements of  $-0.5s$  and  $+0.5s$  were not statistically significant, for both tumor and normal tissue; this was also evident for  $T_1$  displacement of  $-1.0s$ , except for MTT for tumor. No significant impact on BF values was evident for the full range in  $T_1$  from  $-2s$  to  $+2s$ . In general, positive shifts in  $T_1$  (i.e.  $+1s$  and  $+2s$ ) had more detrimental effects on CTP parameter values than corresponding negative shifts in  $T_1$  (i.e.  $-1s$  and  $-2s$ ).



Formal statistical comparisons of tumor and normal liver were not undertaken since this was not a specific objective of this work. However, our results qualitatively indicate that the range of values for BF, BV and PS for tumor were larger than for normal liver (Figure 3). BF and HAF for tumor were generally higher than for normal liver, and conversely for MTT and PS.

## DISCUSSION

This work was undertaken to investigate the impact of one factor that can potentially influence CTP analyses and resultant CTP parameter values, namely, delineation of the pre-enhancement setpoint. In CTP analytical software, this is a user-defined parameter and there is inevitably the potential for observer variations, as borne out in our pilot study of observer variability in pre-enhancement setpoints described above. Noise and artifacts in the acquired data are some of the reasons that likely contribute to the variability. Delineation of the  $T_1$  setpoint potentially impacts on characterization of the vascular input functions as well as baseline tissue Hounsfield density values.

Our previous work demonstrated that CTP parameter values can vary with acquisition durations, and it was found that the parameter values approached steady-state values with increasing acquisition times.<sup>30</sup> Our current analysis suggests that this pattern of behavior was not affected by the various pre-enhancement displacements within the range assessed. The levels of confidence in stabilization of CTP parameters attained by specific acquisition durations were substantially the same for the various pre-enhancement displacements evaluated.

Our results, however, indicate that the *absolute* values of CTP parameter can be affected by the positioning of the pre-enhancement setpoint. It would be excessively complex to present multiple analyses related to all, or indeed several combinations, of pre-enhancement setpoints and acquisition durations. For simplicity, we undertook comparative analyses at two representative acquisition durations, specifically at times when at least moderate and high levels of confidence in stability for the majority of the CTP parameters were attained, namely, 220s and 360s, respectively. The magnitude and statistical significance of the effects, compared to corresponding reference values (at  $T_1=0s$ ), varied according to the CTP parameter. The effects on BF were relatively small (range  $\pm 5\%$ ) and were not significant across the range of pre-enhancement setpoints evaluated ( $-2s$  to  $+2s$ ), for both tumor and normal liver. There were negligible differences in the overall statistical outcomes when comparing the 220s and 360s groups; there was only one exception, that of BV in normal liver at  $-2.0s$ , where a significant difference was evident at 220s but not at 360s. This is probably a reflection of the greater variability in parameter values at the lower level of stabilization associated with 220s compared to 360s.

Overall, displacements in pre-enhancement setpoints of  $\pm 0.5s$  did not have significant effects on absolute values of CTP parameters, for both tumor and normal liver. This was also evident for  $-1.0s$  displacement, with the single exception of MTT for tumor. In general, positive displacements in  $T_1$  greater than or equal to  $+1.0s$  were more deleterious than corresponding negative displacements, when comparing the impact on differences in CTP

values in relation to reference values. Our pilot assessment of observer variability in  $T_1$  positioning indicated that in practice displacement of  $\pm 0.5s$  are common; fortuitously, the current results suggest that such displacements are unlikely to be detrimental to resultant CTP values. Our results further suggest that in practice, if there is uncertainty about the delineation of the pre-enhancement setpoint, one would be better advised to err on the side of negative, rather than positive, positioning of  $T_1$ .

There have been relatively few studies which have examined the effects of pre-enhancement setpoints on CTP parameter values using the same underlying physiological model as in our study i.e. the distributed parameter model. Sanelli et al. in a study of 3 patients with suspected cerebrovascular events, using the brain perfusion protocol of the model, have reported that the positioning of this user-defined variable can significantly influence CTP parameter values,<sup>27</sup> as we have found. In practice, delineation of the correct or appropriate  $T_1$  can be challenging if there is noise in the vascular (arterial) time-attenuation curve, a relatively shallow rise in the arterial up-slope and/or a short pre-enhancement time interval to assess baseline values. Development of algorithms to help identify  $T_1$  reliably and consistently would likely be helpful.<sup>31</sup>

As regards comparison of tumor and normal liver, both had broadly similar patterns of behavior with respect to stabilization in CTP values with acquisition duration. The required acquisition times to achieve low, moderate and high confidence in stabilization for each CTP parameter were also broadly similar for both tumor and normal liver. There was a noticeably wider range of BF, BV and PS values amongst the tumor group compared to normal tissue. This is probably a reflection of the greater heterogeneity amongst tumors, even of a single histological type, than amongst normal liver.

In this work, we principally investigated the effect of pre-enhancement setpoint on resultant CTP parameter values. We have found that the former can significantly affect parameter values. However, as noted in other studies, the post-enhancement setpoint, or acquisition duration, can also significantly affect CTP parameter values.<sup>10,13,30,32</sup> The interaction of these two variables in determining CTP parameter values is complex, and for simplicity, we undertook formal comparative analyses at only a limited number of acquisition durations. In principle, similar analyses could be undertaken with multiple other combinations of acquisition durations and pre-enhancement setpoints.

We recognize and acknowledge several limitations in our study. We had a relatively small number of patients. Our study was limited only to the liver and metastases to the liver from one specific tumor. The extent to which our conclusions might be generalizable to other tissues and tumors would require further work.

We recognize that different versions of CT Perfusion software may generate different results.<sup>33</sup> In our analysis, we used a more current version of software (GE CT Perfusion 4) than the previous work of Sanelli et al.<sup>27</sup> An evaluation of the impact of the differing software versions or of other physiological models on our main objectives was beyond the scope of this work.



In summary, CTP parameter values were affected by the positioning of the pre-enhancement setpoint. The impact on parameter values varied by the specific CTP parameter, with BF being the least sensitive to variations in positioning of  $T_1$ . Significant effects on CTP parameter values were generally evident with positive displacements of  $T_1$ , relative to the reference position, of 1s or more, and negative displacements of 2s or more. Further work is required to determine to what extent our results are generalizable to other tissues, acquisition protocols, and other analysis software.

## Acknowledgments

Research funding: This work was generously supported in part by Genentech and Novartis

## REFERENCES

1. Miles KA, Charnsangavej C, Lee FT, et al. Application of CT in the investigation of angiogenesis in oncology. *Acad. Radiol.* 2000; 7:840–850. [PubMed: 11048881]
2. Miles KA. Functional computed tomography in oncology. *Eur. J. Cancer.* 2002; 38:2079–2084. [PubMed: 12387833]
3. Miles KA, Griffiths MR. Perfusion CT: a worthwhile enhancement? *Br. J. Radiol.* 2003; 76:220–231. [PubMed: 12711641]
4. Kambadakone AR, Sahani DV. Body perfusion CT: technique, clinical applications, and advances. *Radiol. Clin. North Am.* 2009; 47:161–178. [PubMed: 19195541]
5. Gandhi D, Hoeffner EG, Carlos RC, et al. Computed tomography perfusion of squamous cell carcinoma of the upper aerodigestive tract. Initial results. *J. Comput. Assist. Tomogr.* 2003; 27:687–693.
6. Bisdas S, Baghi M, Wagenblast J, et al. Differentiation of benign and malignant parotid tumors using deconvolution-based perfusion CT imaging: feasibility of the method and initial results. *Eur. J. Radiol.* 2007; 64:258–265. [PubMed: 17399933]
7. Makari Y, Yasuda T, Doki Y, et al. Correlation between tumor blood flow assessed by perfusion CT and effect of neoadjuvant therapy in advanced esophageal cancers. *J. Surg. Oncol.* 2007; 96:220–229. [PubMed: 17450532]
8. Bellomi M, Petralia G, Sonzogni A, et al. CT perfusion for the monitoring of neoadjuvant chemotherapy and radiation therapy in rectal carcinoma: initial experience. *Radiology.* 2007; 244:486–493. [PubMed: 17641369]
9. Goh V, Halligan S, Hugill JA, et al. Quantitative assessment of colorectal cancer perfusion using MDCT: inter- and intraobserver agreement. *Am. J. Roentgenol.* 2005; 185:225–231. [PubMed: 15972428]
10. Goh V, Halligan S, Hugill JA, et al. Quantitative colorectal cancer perfusion measurement using dynamic contrast-enhanced multidetector-row computed tomography: effect of acquisition time and implications for protocols. *J. Comput. Assist. Tomogr.* 2005; 29:59–63. [PubMed: 15665684]
11. Goh V, Liaw J, Bartram CI, et al. Effect of temporal interval between scan acquisitions on quantitative vascular parameters in colorectal cancer: implications for helical volumetric perfusion CT techniques. *Am. J. Roentgenol.* 2008; 191:W288–292. [PubMed: 19020217]
12. Jensen N, Lock M, Kozak R, et al. SU-GG-I-101: 3D segmentation and rigid registration for minimizing breathing motion effects in liver CT perfusion. *Med. Phys.* 2010; 37:3124.
13. Kambadakone AR, Sharma A, Catalano OA, et al. Protocol modifications for CT perfusion (CTp) examinations of abdomen-pelvic tumors: impact on radiation dose and data processing time. *Eur. Radiol.* 2011; 21:1293–1300. [PubMed: 21246200]
14. Sahani DV, Kalva SP, Hamberg LM, et al. Assessing tumor perfusion and treatment response in rectal cancer with multisection CT: initial observations. *Radiology.* 2005; 234:785–792. [PubMed: 15734934]

15. Xu K, Xiao Z-W, et al. Peripheral lung cancer: relationship between multi-slice spiral CT perfusion imaging and tumor angiogenesis and cyclin D1 expression. *Clin. Imaging.* 2007; 31:165–177. [PubMed: 17449377]
16. Wang J, Wu N, Cham MD, et al. Tumor response in patients with advanced non-small cell lung cancer: perfusion CT evaluation of chemotherapy and radiation therapy. *Am. J. Roentgenol.* 2009; 193:1090–1096. [PubMed: 19770333]
17. Ng CS, Chandler AG, Wei W, et al. Reproducibility of perfusion parameters obtained from perfusion CT in lung tumors. *Am. J. Roentgenol.* 2011; 197:113–121. [PubMed: 21701018]
18. Onofrio M, Gallotti A, Mantovani W, et al. Perfusion CT can predict tumoral grading of pancreatic adenocarcinoma. *Eur. J. Radiol.* 2013; 82:227–233. [PubMed: 23127804]
19. Klauss M, Stiller W, Pahn G, et al. Dual-energy perfusion-CT of pancreatic adenocarcinoma. *Eur. J. Radiol.* 2013; 82:208–214. [PubMed: 23062281]
20. Sahani DV, Holalkere N-S, Mueller PR, et al. Advanced hepatocellular carcinoma: CT perfusion of liver and tumor tissue--initial experience. *Radiology.* 2007; 243:736–743. [PubMed: 17517931]
21. Zhu AX, Holalkere NS, Muzikansky A, et al. Early antiangiogenic activity of bevacizumab evaluated by computed tomography perfusion scan in patients with advanced hepatocellular carcinoma. *Oncologist.* 2008; 13:120–125. [PubMed: 18305056]
22. Zhang Q, Yuan ZG, Wang DQ, et al. Perfusion CT findings in liver of patients with tumor during chemotherapy. *World J. Gastroenterol.* 2010; 16:3202–3205. [PubMed: 20593507]
23. Kanda T, Yoshikawa T, Ohno Y, et al. CT hepatic perfusion measurement: Comparison of three analytic methods. *Eur. J. Radiol.* 2011
24. Lawrence KS, Lee TY. An adiabatic approximation to the tissue homogeneity model for water exchange in the brain: II. Experimental validation. *J. Cereb. Blood Flow Metab.* 1998; 18:1378–1385. [PubMed: 9850150]
25. Lee TY. Functional CT: physiological models. *Trends Biotechnol.* 2002; 20:S3–S10. [PubMed: 12570152]
26. Stewart EE, Chen X, Hadway J, et al. Hepatic perfusion in a tumor model using DCE-CT: an accuracy and precision study. *Phys. Med. Biol.* 2008; 53:4249–4267. [PubMed: 18653923]
27. Sanelli PC, Lev MH, Eastwood JD, et al. The effect of varying user-selected input parameters on quantitative values in CT perfusion maps. *Acad. Radiol.* 2004; 11:1085–1092. [PubMed: 15530801]
28. Chandler A, Wei W, Herron DH, et al. Semiautomated motion correction of tumors in lung CT-perfusion studies. *Acad. Radiol.* 2011; 18:286–293. [PubMed: 21295733]
29. Chandler A, Wei W, Anderson EF, et al. Validation of motion correction techniques for liver CT perfusion studies. *Br. J. Radiol.* 2012
30. Ng CS, Hobbs BP, Chandler AG, et al. Effect of duration of scan acquisition on CT perfusion values in metastases to the liver from neuroendocrine tumors and in normal liver. *Radiology.* (in press).
31. Soares BP, Dankbaar JW, Bredno J, et al. Automated versus manual post-processing of perfusion-CT data in patients with acute cerebral ischemia: influence on interobserver variability. *Neuroradiology.* 2009; 51:445–451. [PubMed: 19274457]
32. Yeung TP, Yartsev S, Bauman G, et al. The effect of scan duration on the measurement of perfusion parameters in CT perfusion studies of brain tumors. *Acad. Radiol.* 2013; 20:59–65. [PubMed: 23085409]
33. Goh V, Shastry M, Engledow A, et al. Commercial software upgrades may significantly alter Perfusion CT parameter values in colorectal cancer. *Eur. Radiol.* 2011; 21:744–749. [PubMed: 20922392]

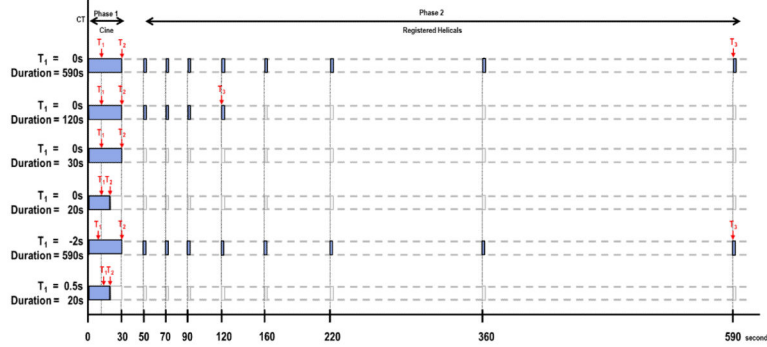


**FIGURE 1. Schematic of overall study evaluating effects of acquisition duration and pre-enhancement setpoints.**

First row: Reference dataset: Phase 1, combined with 8 anatomically registered Phase 2 images.  $T_1$ , pre-enhancement setpoint;  $T_2$ , last first phase setpoint;  $T_3$ , last second phase (“post-enhancement”) setpoint.

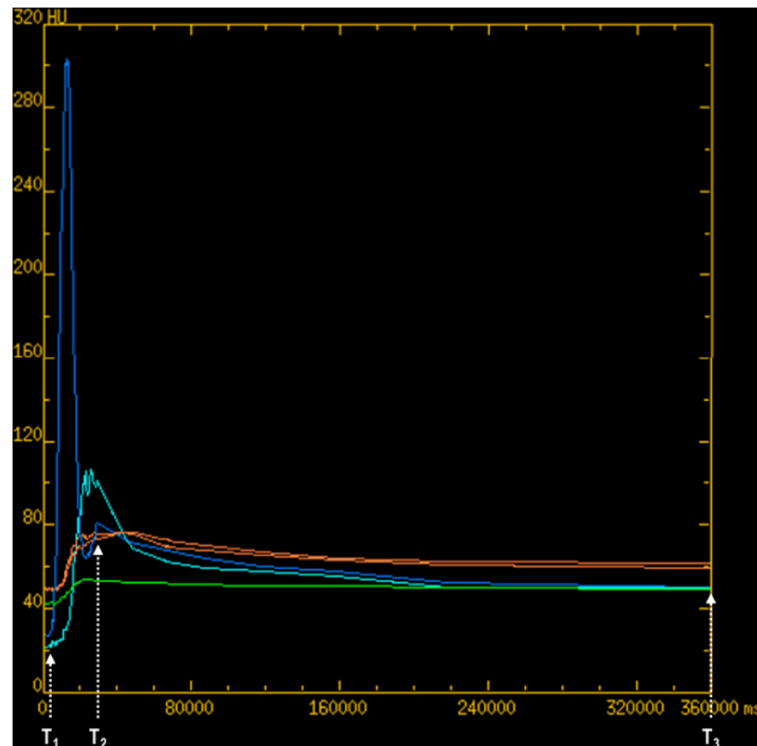
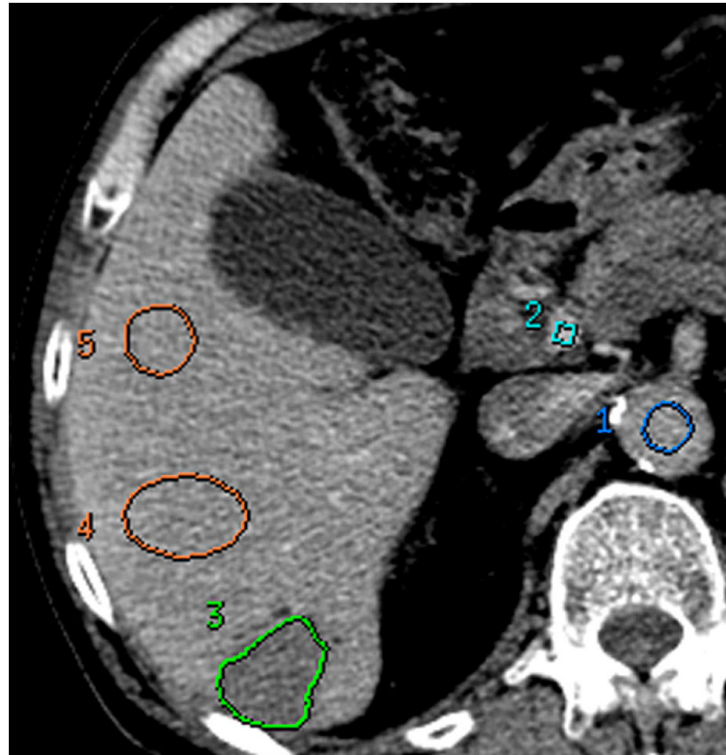
Second row: Reduction in acquisition duration affecting Phase 2 ( $T_3$ ).

Third row: Reduction in acquisition duration,  $T_2=30s$ .

Fourth row: Reduction in acquisition duration affecting Phase 1 ( $T_2$ ).

Fifth row: Displacement of pre-enhancement setpoint:  $T_1$  displacement backwards in increments ( $-0.5s$ ,  $-1.0s$ ,  $-2.0s$ ). Analyses of 2<sup>nd</sup>, 3<sup>rd</sup> and 4<sup>th</sup> rows were repeated.

Sixth row: Displacement of pre-enhancement setpoint:  $T_1$  displacement forwards in increments ( $+0.5s$ ,  $+1.0s$ ,  $+2.0s$ ). Analyses of 2<sup>nd</sup>, 3<sup>rd</sup> and 4<sup>th</sup> rows were repeated.



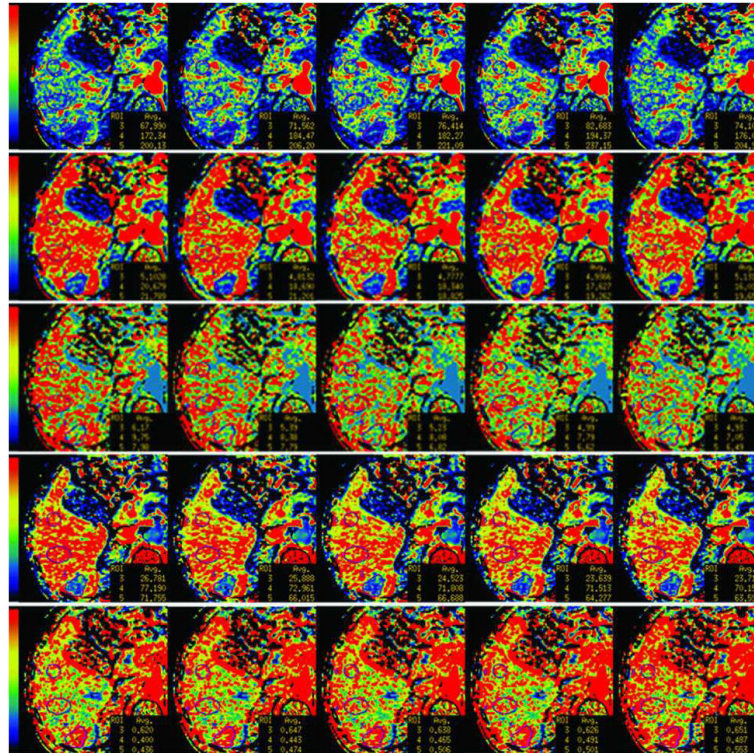


**FIGURE 2. 70 year old male with metastatic carcinoid to the liver**

(a): reference CTp image with tissue ROIs, (b) corresponding time-attenuation curves.

Aortic and portal vein (dark blue and light blue respectively), tumor (green), and normal liver (orange). X-axis in milliseconds.

(c) Parametric maps for BF, BV, MTT, PS and HAF (first to fifth rows, respectively) with illustrative examples of pre-enhancement setpoints at  $-2.0s$ ,  $-0.5s$ ,  $0s$  (reference),  $+0.5s$ ,  $+2.0s$  (left to right columns, respectively). BF, in mL/min/100g; BV, in mL/100g; MTT, in seconds; PS, in mL/min/100g; HAF, unitless. The color scales are identical for individual rows of parametric maps. Differences in maps can be seen when comparing left-hand columns and right-hand columns.

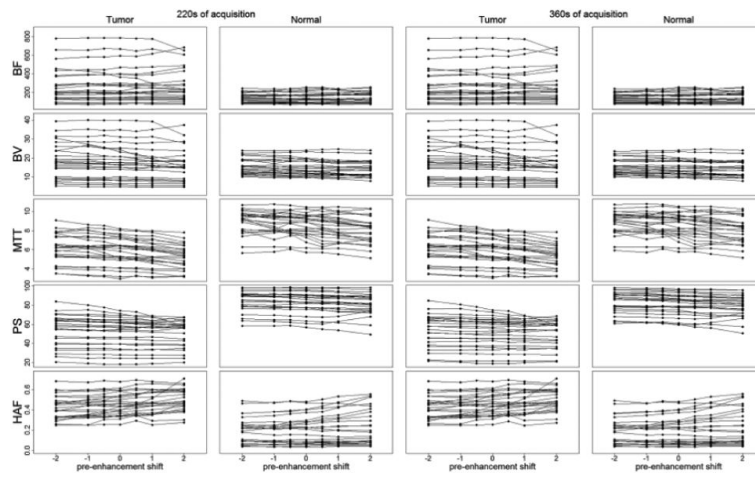


**FIGURE 3.** Mean CTP parameter values at varying pre-enhancement setpoints, after 220s (left-hand columns) and 360s (right-hand columns) of acquisition. Solid lines connect CTP values observed within the same ROI.  
 y-axes: BF, in mL/min/100g; BV, in mL/100g; MTT, in seconds; PS, in mL/min/100g; HAF, unitless.



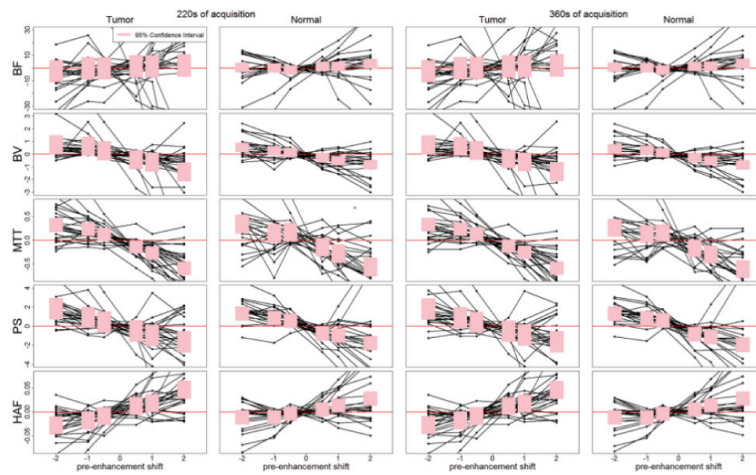


**FIGURE 4.**

Deviation of CTp parameter values from reference at  $T_1 = 0s$  as a function of displacement in pre-enhancement setpoints. Solid lines connect deviations observed within the same ROI. Shaded pink regions correspond to 95% confidence intervals for the displacement effects; over-lapping of the shaded regions with the horizontal red line indicates non-significant deviation from the reference pre-enhancement setpoint of  $T_1=0s$ . Plots presented for 220s (two left-hand columns) and 360s (two right-hand columns). y-axes: BF, in mL/min/100g; BV, in mL/100g; MTT, in seconds; PS, in mL/min/100g; HAF, unitless.



**TABLE 1**

Level of confidence in stability of CTP parameter values as a function of acquisition duration, and three levels of pre-enhancement displacement, observed in liver tumors and normal liver tissue. (Note: PS failed to stabilize with high confidence within the 590s of available data).

T <sub>1</sub> time relative to T <sub>1</sub> =0s (seconds)	CTp parameter	Tumor				Normal liver			
		160s	220s	360s	590s	160s	220s	360s	590s
-2.0s	BF	Low	Mod	High	High	Low	Mod	High	High
	BV	Low	Mod	High	High	Low	Mod	High	High
	MTT	Low	Mod	High	High	Low	Mod	High	High
	PS	Low	Low	Mod	Mod	Low	Low	Mod	Mod
	HAF	High	High	High	High	Low	Mod	High	High
0s	BF	Low	Mod	High	High	Low	Mod	High	High
	BV	Low	Mod	High	High	Low	Mod	High	High
	MTT	Low	Mod	High	High	Low	Low	High	High
	PS	Low	Low	Mod	Mod	Low	Low	Mod	Mod
	HAF	-	Mod	High	High	Low	Mod	High	High
+2.0s	BF	Low	Mod	High	High	Low	Mod	High	High
	BV	Low	Mod	High	High	Low	Mod	High	High
	MTT	Low	Mod	High	High	Low	Mod	High	High
	PS	Low	Low	Mod	Mod	Low	Low	Mod	Mod
	HAF	Low	Mod	High	High	Low	Mod	High	High

**TABLE 2**

Summary of the raw CTP values for the reference pre-enhancement setpoint ( $T_1=0s$ ) observed after 220s and 360s of acquisition. BF, in mL/min/100g; BV, in mL/100g; MTT, in seconds; PS, in mL/min/100g; HAF, unitless.

CTp parameter	220s				360s			
	Tumor		Normal liver		Tumor		Normal liver	
	Median	Inter-quartile range	Median	Inter-quartile range	Median	Inter-quartile range	Median	Inter-quartile range
BF	203	139 – 363	134	94 – 175	204	139 – 362	134	94 – 175
BV	16.6	9.9 – 23.1	14.6	11.8 – 18.6	16.6	9.9 – 23.0	14.6	11.8 – 18.6
MTT	6.1	5.1 – 7.2	8.9	7.5 – 9.5	6.2	5.1 – 7.1	8.9	7.8 – 9.5
PS	56.6	39.4 – 62.1	82.9	77.4 – 90.0	55.4	42.7 – 62.7	82.9	74.3 – 89.3
HAF	0.43	0.36 – 0.54	0.210	0.08 – 0.29	0.43	0.36 – 0.53	0.21	0.08 – 0.29

**TABLE 3**

Summaries of the effects of pre-enhancement positioning on CTp parameter values. The analyses considered parameter values after acquisition durations of 220s and 360s. The mean percentage change from pre-enhancement setpoint ( $T_1=0s$ ) and the corresponding 95% confidence intervals derived from the mixed-effects inference are provided in the table.

CTp parameter	$T_1$ time relative to $T_1=0s$ (seconds)	220s				360s			
		Tumor		Normal liver		Tumor		Normal liver	
		Mean (%)	95% CI (%)	Mean (%)	95% CI (%)	Mean (%)	95% CI (%)	Mean (%)	95% CI (%)
BF	-2.0	-1.1	-4.9 – 2.8	0.4	-2.1 – 2.9	-1.2	-5.0 – 2.7	0.5	-2.0 – 3.0
	-1.0	-0.1	-4.0 – 3.8	0.2	-2.3 – 2.7	-0.1	-3.9 – 3.9	0.4	-2.1 – 2.9
	-0.5	-0.1	-3.9 – 3.9	-1.0	-3.5 – 1.5	0.0	-3.9 – 3.9	-1.0	-3.5 – 1.5
	+0.5	0.6	-3.3 – 4.5	1.0	-1.5 – 3.5	0.6	-3.2 – 4.6	1.0	-1.5 – 3.5
	+1.0	0.6	-3.3 – 4.5	1.1	-1.5 – 3.6	0.7	-3.2 – 4.6	1.1	-1.4 – 3.7
	+2.0	0.9	-2.9 – 4.9	2.5	0.0 – 5.1	1.0	-2.9 – 4.9	2.6	0.0 – 5.2
BV	-2.0	4.3	0.2 – 8.8	3.6	1.4 – 6.0	4.3	0.0 – 8.9	2.9	0.6 – 5.3
	-1.0	3.6	-0.5 – 8.1	1.9	-0.4 – 4.2	3.6	-0.5 – 8.1	2.1	-0.2 – 4.4
	-0.5	1.6	-2.4 – 6.0	0.9	-1.4 – 3.2	1.8	-2.2 – 6.1	0.8	-1.5 – 3.0
	+0.5	-2.3	-6.5 – 1.8	-1.8	-4.0 – 0.4	-2.1	-6.3 – 2.0	-1.7	-4.0 – 0.5
	+1.0	-3.6	-7.8 – 0.5	-3.4	-5.6 – -1.1	-3.5	-7.7 – 0.6	-3.3	-5.6 – -1.1
	+2.0	-8.0	-12.7 – -3.9	-5.4	-7.7 – -3.1	-7.9	-12.7 – -3.8	-5.5	-7.9 – -3.3
MTT	-2.0	5.4	3.1 – 7.9	4.0	1.8 – 6.3	5.6	3.3 – 8.1	3.1	1.0 – 5.3
	-1.0	3.9	1.6 – 6.4	1.8	-0.4 – 4.0	4.0	1.7 – 6.4	1.5	-0.5 – 3.7
	-0.5	2.1	-0.2 – 4.5	2.0	-0.2 – 4.3	2.3	0.1 – 4.6	1.7	-0.3 – 3.9
	+0.5	-2.3	-4.6 – -0.1	-1.7	-3.9 – 0.5	-2.0	-4.2 – 0.2	-2.0	-4.0 – 0.1
	+1.0	-4.6	-6.9 – -2.3	-3.3	-5.5 – -1.1	-4.4	-6.7 – -2.1	-3.5	-5.6 – -1.4
	+2.0	-10.1	-12.6 – -7.7	-6.7	-8.9 – -4.5	-10.0	-12.5 – -7.7	-7.1	-9.2 – -5.1
PS	-2.0	3.5	1.4 – 5.8	1.6	0.8 – 2.5	3.5	1.4 – 5.7	1.6	0.7 – 2.6
	-1.0	1.8	-0.3 – 3.9	1.0	0.2 – 1.9	1.7	-0.3 – 3.9	1.0	0.1 – 1.9
	-0.5	0.8	-1.2 – 3.0	0.7	-0.2 – 1.6	0.8	-1.2 – 2.9	0.7	-0.2 – 1.6
	+0.5	-1.0	-3.0 – 1.1	-0.9	-1.8 – 0.0	-1.0	-3.1 – 1.1	-1.0	-1.9 – -0.1
	+1.0	-1.8	-3.9 – 0.2	-1.2	-2.0 – -0.3	-1.8	-3.9 – 0.3	-1.4	-2.3 – -0.5
	+2.0	-3.2	-5.3 – 1.1	-2.1	-3.0 – -1.3	-3.1	-5.3 – -1.1	-2.4	-3.3 – -1.5
HAF	-2.0	-5.9	-9.8 – -2.0	-5.3	-13.0 – 1.8	-5.8	-9.6 – -1.9	-5.2	-12.9 – 1.8
	-1.0	-3.7	-7.6 – 0.2	-5.4	-13.2 – 1.6	-3.7	-7.5 – 0.2	-5.8	-13.5 – 1.3
	-0.5	-1.7	-5.6 – 2.2	-1.4	-8.6 – 5.9	-1.9	-5.7 – 2.1	-1.4	-8.7 – 6.0
	+0.5	2.9	-1.0 – 7.0	3.2	-3.9 – 11.3	2.9	-1.0 – 6.9	3.2	-3.8 – 11.3
	+1.0	4.2	0.3 – 8.3	7.4	0.1 – 16.3	4.1	0.2 – 8.2	7.2	0.1 – 16.2
	+2.0	10.3	6.2 – 14.8	14.8	6.8 – 26.0	10.3	6.2 – 14.7	14.9	6.8 – 26.0

P-values for inference on the effects of pre-enhancement positioning on CTP parameter values. Each p-value corresponds to a two-sided test for the absence of deviation in resultant CTP values from the reference set point ( $T_1=0s$ ) at a given shift from  $T_1$  ( $T_1 = \pm 0.5s, \pm 1.0s, \pm 2.0s$ ). Boldface values represent statistically significant differences after adjusting for multiple comparisons using Bonferroni's correction. The Table shows that the pattern of results is essentially the same for 220s and 360s.

**TABLE 4**

Table 4a: 220s acquisition duration												
	Tumor					Normal						
	-2.0s	-1.0s	-0.5s	0.5s	1.0s	2.0s	-2.0s	-1.0s	-0.5s	0.5s	1.0s	2.0s
BF	0.571	0.942	0.966	0.773	0.781	0.655	0.771	0.898	0.419	0.449	0.416	0.054
BV	0.043	0.091	0.443	0.259	0.084	<0.001	<b>0.002</b>	0.104	0.445	0.114	<b>0.004</b>	<0.001
MTT	<0.001	<b>0.001</b>	0.073	0.046	<0.001	<0.001	<0.001	0.117	0.078	0.121	<b>0.003</b>	<0.001
PS	<b>0.001</b>	0.098	0.448	0.366	0.085	<b>0.004</b>	<0.001	0.022	0.115	0.042	<b>0.008</b>	<0.001
HAF	<b>0.004</b>	0.064	0.374	0.147	0.039	<0.001	0.142	0.134	0.677	0.391	0.047	<0.001

Table 4b: 360s acquisition duration												
	Tumor					Normal						
	-2.0s	-1.0s	-0.5s	0.5s	1.0s	2.0s	-2.0s	-1.0s	-0.5s	0.5s	1.0s	2.0s
BF	0.544	0.956	0.984	0.766	0.753	0.639	0.726	0.784	0.419	0.444	0.387	0.045
BV	0.042	0.091	0.403	0.300	0.094	<0.001	0.013	0.070	0.511	0.133	<b>0.004</b>	<0.001
MTT	<0.001	<b>0.001</b>	0.045	0.079	<0.001	<0.001	<b>0.004</b>	0.151	0.104	0.066	<b>0.001</b>	<0.001
PS	<b>0.001</b>	0.106	0.459	0.352	0.090	<b>0.003</b>	<0.001	0.030	0.113	0.023	<b>0.003</b>	<0.001
HAF	<b>0.004</b>	0.065	0.348	0.151	0.041	<0.001	0.146	0.110	0.689	0.391	0.050	<0.001